



# 1 Diurnal and day-to-day characteristics of ambient particle mass size 2 distributions from HR-ToF-AMS measurements at an urban site and 3 a suburban site in Hong Kong

4 Berto P. Lee<sup>1</sup>, Hao Wang<sup>2</sup>, and Chak K. Chan<sup>1,2\*</sup>

5 <sup>1</sup>School of Energy and Environment, City University of Hong Kong, Hong Kong, China

6 <sup>2</sup>Division of Environment, Hong Kong University of Science and Technology, Hong Kong, China

7 *Correspondence to:* Chak K. Chan (chak.k.chan@cityu.edu.hk)

8 **Abstract.** Mass concentration based particle size distributions measured by a high-resolution aerosol mass spectrometer were  
9 systematically analyzed to assess long and short-term temporal characteristics of ambient particle size distributions sampled  
10 at a typical urban environment close to emission sources and a suburban coastal site representing a regional and local pollution  
11 receptor location in Hong Kong. Measured distributions were bimodal and deconvoluted into submodes which were analyzed  
12 for day-to-day variations and diurnal variations. Traffic and cooking emissions at the urban site contributed substantially to  
13 particle mass in both modes, while notable decreases in mass median diameters were limited to the morning rush hour.  
14 Inorganic particle components displayed varying diurnal behavior, including nocturnal nitrate formation and daytime  
15 photochemical formation evident in both modes. Suburban particle size distributions exhibited notable seasonal disparities  
16 with differing influence of local formation, particularly in spring and summer, and transport which dominated in the fall season  
17 leading to notably higher sulfate and organic accumulation mode particle concentrations. Variations in particle mixing state  
18 were evaluated by comparison of inter-species mass median diameter trends at both measurement sites. Internal mixing was  
19 prevalent in the accumulation mode in spring at the urban site, while greater frequency of time periods with external mixing  
20 of particle populations comprising different fractions of organic constituents was observed in summer. At the suburban site,  
21 sulfate and nitrate in the accumulation mode more frequently exhibited differing particle size distributions in all seasons  
22 signifying a greater extent of external mixing. At the urban site, periods of greater submicron inorganic mass concentrations  
23 were more likely to be caused by increases in both Aitken and accumulation mode particle mass in summer, while at the  
24 suburban receptor location organic and nitrate Aitken mode particle mass contributed more regularly to higher total submicron  
25 species mass concentrations in most seasons (spring, summer and winter).



## 26 1. Introduction

27 Apart from mass and chemical composition, the size distribution of fine particles represents a vital physical property with  
28 important implications for human health and environmental effects of ambient aerosols [Seinfeld and Pandis, 2006]. Particle  
29 size relates directly to the aerodynamic properties which govern the penetration and deposition of particles in the airways and  
30 lungs [Davidson *et al.*, 2005] as well as the scattering and absorption of light which affect the radiative properties and hence  
31 ambient visibility [Ahlquist and Charlson, 1967; Bohren and Huffman, 1983; Charlson *et al.*, 1991; Schwartz, 1996; Seinfeld  
32 and Pandis, 2006]. Hygroscopic growth in response to changes in ambient humidity can alter particle light scattering properties  
33 (Seinfeld and Pandis, 2006; Köhler, 1936) and activation of condensation nuclei particles into cloud droplets depend on  
34 atmospheric conditions, chemical composition, mixing state as well as the size and morphology of particles (Abbatt *et al.*,  
35 2005; Kerminen *et al.*, 2012; Meng *et al.*, 2014; Westervelt *et al.*, 2013).

36 Studies into the size distribution of ambient particulate matter in Hong Kong have been largely based on size-segregated filter  
37 samples (Yao *et al.*, 2007b; Zheng *et al.*, 2008; Zhuang *et al.*, 1999; Huang *et al.*, 2014; Bian *et al.*, 2014) and measurements by  
38 electrostatic classifier instruments (Cheung *et al.*, 2015; Yao *et al.*, 2007a) and were hence either limited in size resolution  
39 (offline filter samples) or chemical resolution (total particle count by classification). The majority of measurements in Hong  
40 Kong were conducted in suburban environments. Inorganic ammonium and sulfate were mainly found in fine mode particles  
41 in condensation and droplet mode size ranges, while nitrate had strong coarse mode contributions (Zhuang *et al.*, 1999).  
42 Seasonal differences were evident in solvent-extractable organics and trace metals which were mainly found in PM<sub>0.5</sub> particles  
43 in the wet season and winter whereas in fall a shift to larger particles (0.5–2.5 μm fraction) in fall indicated a possibly stronger  
44 influence of aged particle components in the transition period of the Asian monsoon (Zheng *et al.*, 2008). Size distributions  
45 acquired by a fast mobility particle sizer at the suburban HKUST supersite were investigated more recently to study the  
46 formation and accumulation of ultrafine particles under different air flow regimes. Particle number concentration  
47 enhancements during the day were attributed to secondary formation, while evening and nighttime peaks were thought to be  
48 related to transport of aged aerosols from upwind locations. Nucleation mode particle peaks were often observed in fall and  
49 related to regional pollution influence (Cheung *et al.*, 2015). New particle formation events at the same site occurred as single  
50 and two-stage growth processes with organics and sulfuric acid contributing mainly to first stage growth in the daytime while  
51 nighttime second stage growth was attributed to ammonium nitrate and organics. Particle size growth into the diameter range  
52 of cloud condensation nuclei (CCN) was typically only achieved with the second growth stage (Man *et al.*, 2015).

53 Investigations into particle size distributions in urban areas of Hong Kong are even scarcer. Yao *et al.* (Yao *et al.*, 2007a)  
54 studied the properties and behavior of particles in vehicle plumes and reported a competing process between ambient  
55 background particles and fresh soot particles in the condensation of gaseous precursors and a dependency on temperature with  
56 bimodal volume size distributions observed at lower ambient temperatures and unimodal distributions in the lower  
57 accumulation size range at higher ambient temperatures.



58 The Aerodyne aerosol mass spectrometer (Canagaratna et al., 2007) is widely used to determine the chemical composition of  
59 major organic and inorganic components of non-refractory submicron particulate matter (NR-PM<sub>1</sub>). In contrast to most  
60 traditional aerosol sizing instruments, the AMS is capable of resolving main chemical constituents within size distributions  
61 through analysis of particle flight times and particle ensemble mass spectra [Canagaratna et al., 2007; Jayne et al., 2000;  
62 Jimenez et al., 2003; Rupakheti et al., 2005] and thus yields valuable additional information on differences in composition of  
63 submicron particles with the gross of particle mass in the Aitken mode range ( $D_p \sim 10\text{-}100\text{nm}$ ) and the accumulation mode  
64 range ( $D_p \sim 100\text{-}1000\text{nm}$ ) covered by the AMS. Despite the potentially different chemical and physical processes affecting  
65 species in different size regions within NR-PM<sub>1</sub>, AMS particle size data from ambient measurements are rarely investigated  
66 in-depth. Thus, in this work we demonstrate a systematic approach to analyzing AMS species-segregated mass-based particle  
67 size distributions and present a detailed discussion of particle size data from HR-ToF-AMS measurements during two field  
68 campaigns in Hong Kong in both urban and suburban environments. We aim to evaluate characteristic recurrent changes in  
69 size distribution as well as longer term trends in different seasons by analyzing day-to-day variations and diurnal variations of  
70 size distributions of submicron organics, sulfate, and nitrate particle mass. Two contrasting sites were chosen representing a  
71 typical urban source environment (inner-city, roadside station) close to primary emission sources and a suburban location  
72 (coastal, HKUST supersite) which is largely a downwind receptor of varying amounts of local urban, regional and long-range  
73 transported pollutants (Li et al., 2015;Huang et al., 2014).

## 74 2. Methodology

### 75 2.1. Field campaigns

76 Sampling of ambient submicron non-refractory particulate matter (NR-PM<sub>1</sub>) was carried out using an Aerodyne HR-ToF-AMS  
77 at the HKUST air quality supersite covering four seasons between May 2011 and February 2012 (spring: 2011-05, summer:  
78 2011-09, fall: 2011-11&12, winter: 2012-02). The HKUST supersite is located on the campus of the Hong Kong University  
79 of Science and Technology (22°20'N, 114°16'E), on the east coast of Hong Kong in a suburban area with few primary emission  
80 sources in the immediate vicinity. Sampled air was drawn from the rooftop of a pump house building at an approximate height  
81 of 25m above ground level. For detailed descriptions of the experimental setup, operating conditions, data treatment, and  
82 overall species composition we refer the reader to previous publications (Lee et al., 2013;Li et al., 2015;Li et al., 2013). A  
83 further sampling campaign took place between spring 2013 (2013-03 to 2013-05) and summer 2013 (2013-05 to 2013-07) at  
84 an inner-city urban location in the densely populated and built-up Kowloon peninsula. Measurements were conducted next to  
85 the roadside air quality monitoring station (AQMS) operated by the Environmental Protection Department (EPD) of the  
86 HKSAR Government in the Mong Kok (MK) district on a pedestrian crossing at a major road junction. Sampled air was drawn  
87 from a height of 3m above ground level. A comprehensive analysis of trends in species concentration and composition  
88 identified in this urban campaign has been presented previously (Lee et al., 2015). In both campaigns, particles were sampled  
89 through a PM<sub>2.5</sub> cyclone at a flow rate of 16.67 L/min into a sampling port from which 0.08 L/min was drawn by the AMS and



90 the remainder drawn by co-sampling instruments and an auxiliary pump. Sample air for the AMS passed through a 1 m long  
91 diffusion dryer (BMI, San Francisco CA, USA) filled with silica gel to remove bulk gas- and particle-phase water. Additional  
92 data from various collocated instruments including meteorological data (wind, temperature, relative humidity, solar  
93 irradiation), volatile organic compounds (VOCs) and standard trace gases such as NO<sub>x</sub>, SO<sub>2</sub>, and O<sub>3</sub> were available and details  
94 on employed instrument models and sampling methodologies are discussed in aforementioned studies (Lee et al., 2013, 2015; Li  
95 et al., 2015; Li et al., 2013).

## 96 2.2. Data acquisition and treatment

97 In both campaigns, mass concentration based size distributions in terms of vacuum-aerodynamic particle diameter  
98 ( $dM/d\log D_{va}$ ) were established by joint acquisition of particle time-of-flight (PToF) measurements and unit mass resolution  
99 mass spectra (V-mode) with alternation between modes every 20s for 30 cycles amounting to 5 min of total sampling time.  
100 High-resolution mass spectra were acquired for the following 5 min, and thus the overall raw data time resolution for each  
101 mode was equal to 10 min. The total particle mass measured in the PToF mode was normalized to the V-mode mass  
102 concentration of the same time step. Daily size distributions were generated by averaging over 24h periods (from 0:00 to  
103 23:59). Hourly diurnal size distributions were reconstructed by grouping size distributions within the same hour of the day and  
104 establishing representative size distributions based on average, median, 25<sup>th</sup> and 75<sup>th</sup> percentile concentration values of each  
105 size bin (*referred to as size distribution sets hereinafter*).

106 At both sampling sites, the seasonally averaged AMS size distributions were bimodal (Lee et al., 2013, 2015; Li et al., 2015)  
107 with similar distributions having been observed in other AMS field studies in various parts of the world. (Zhang et al., 2014; Sun  
108 et al., 2011; Huang et al., 2011; Aiken et al., 2009; Zhang et al., 2005; Crippa et al., 2013; Docherty et al., 2011; Mohr et al.,  
109 2012). Multimodality of size distributions is typical for environments where different sources or formation processes of  
110 particles play a role and accordingly such distributions can also be represented as sums of discrete lognormal distributions of  
111 the respective constituting submodes (John, 2011).

112 The measured bimodal size distributions in this work were therefore deconvoluted by fitting two log-normal distributed modes,  
113 including one closer to the Aitken size range (*mode diameter ~100nm*) and one in the accumulation size range (*mode diameter*  
114 *~500nm*), to evaluate differences in trends and formation or transformation processes in the two size regimes. An example of  
115 a size distribution fit and associated parameters is depicted in Figure D1 in the Supporting Material. Mode diameter (*i.e.* mass  
116 median diameter, MMD), curve width (*i.e.* geometric standard deviation, GSD) and curve area (*equivalent to particle mass*  
117 *concentration within the mode*) are sufficient parameters to completely describe a lognormal distribution and these key  
118 variables are used in the following analysis on trends in the fitted species-specific size distributions of organics, nitrate, and  
119 sulfate from both HR-AMS sampling campaigns in Hong Kong. Particle diameters are discussed in terms of vacuum-  
120 aerodynamic diameter, with detailed discussions on properties and relationships to other size metrics available elsewhere  
121 (DeCarlo et al., 2004; Slowik et al., 2004). Further details on PToF data acquisition and size distribution averaging can also be



122 found in the Supporting Material in Section A and B respectively. While the transmission efficiency of the AMS aerodynamic  
123 lens is known to fall off beyond  $\sim 1 \mu\text{m}$  of vacuum-aerodynamic diameter (Liu et al., 2007; Takegawa et al., 2009; Zhang et al.,  
124 2004; Bahreini et al., 2008) and may bias measured particle mass in the accumulation mode towards lower concentrations,  
125 resolved MMDs at either sampling location were generally well within the upper transmission limit and thus unlikely to have  
126 significant effect on the presented analysis.

### 127 3. Results and Discussion

#### 128 3.1. Diurnal size distribution characteristics

129 Diurnal species variations are predominantly discussed in terms of total mass concentration up to the size cut of the sampling  
130 inlet or the instrumental capability, e.g. total species concentrations in NR-PM<sub>1</sub> for AMS-based studies. Utilizing AMS mass-  
131 based size distributions and their deconvolution provides complementary insights into the variations of different particle size  
132 submodes and their contributions to the overall species variation in NR-PM<sub>1</sub>. As previously mentioned, we examined size  
133 distributions reconstructed from the average, median, 25th and 75th percentile of hourly grouped size distributions, analogous  
134 to commonly reported AMS species diurnal variations, with quantitative analysis focusing on concentrations from the median  
135 dataset.

#### 136 3.2. Urban roadside NR-PM<sub>1</sub>

137 The urban roadside measurements took place between March and July 2013 covering two seasons (Spring 2013: *March to*  
138 *mid-May 2013*; Summer 2013: *mid-May to July 2013*) at a location dominated by the influence of primary emission sources.  
139 Organics were the major particulate species in NR-PM<sub>1</sub> of which two-thirds were attributable to traffic and cooking sources.  
140 Anthropogenic gas-phase species, including various VOCs, NO<sub>x</sub>, CO, and SO<sub>2</sub> were continuously abundant as well (Lee et al.,  
141 2015; Sun et al., 2016). Particle size distributions at the urban site exhibited discernible diurnal trends, with Figure 1 depicting  
142 the variations in (mass median) diameters of the lognormal fitted Aitken and accumulation modes, corresponding integrated  
143 peak areas representing the total mass accounted for by particles in each mode, the geometric standard deviation signifying the  
144 spread across particle sizes as well as the total submicron mass (NR-PM<sub>1</sub>) diurnal variation for organics, sulfate, and nitrate  
145 based on AMS V-mode data. Individual trends are discussed species-wise in the following.

#### 147 Organics

148 The diurnal variation of total Aitken and accumulation mode particle mass both largely followed the same trend as total  
149 submicron organic mass (lower panels in Figure 1 a,b) affirming that urban sources of organic particulate matter contributed  
150 substantially to PM mass across the covered size region. Mass concentrations in both modes were smallest during the the night  
151 (0:00 to 6:00) and highest during lunch and dinner (12:00 to 14:00, 19:00 to 21:00), when the influence of organic aerosol



152 from cooking (COA - cooking organic aerosol) and from traffic (HOA – hydrocarbon-like organic aerosol) were dominant  
153 (Lee et al., 2015). Trends in integrated mode particle mass and MMDs were similar across all size distribution sets (Figure D2  
154 in the Supporting Material), confirming that they occurred persistently throughout the measurement period and making diurnal  
155 timescale processes the dominant factor in determining size characteristics of organic-containing particles at this urban  
156 roadside location.

157 Minimum Aitken mode particle mass concentrations (*median values*) amounted to  $2.3 \mu\text{g}/\text{m}^3$  in spring and  $1.2 \mu\text{g}/\text{m}^3$  in  
158 summer, accounting for 28-38% of total submicron particulate mass, and were typically reached between 03:00 and 04:00.  
159 These concentrations represent the estimated urban background mass of Aitken mode particles carried over from the daytime  
160 and not removed by gravitational settling, coagulation or sweep-out as well as contributions from nighttime activity such as  
161 residual traffic.

162 Organic concentrations increased notably between 6:00 and 9:00 during the morning rush hour with traffic-related constituents  
163 (HOA – hydrocarbon-like organic aerosol) accounting for the largest part (60% in spring, 40% in summer) of this increase  
164 (Table A1 in the Supporting Material). In the Aitken mode, particle mass concentrations rose by  $1.6 \mu\text{g m}^{-3}$  (spring) and  $0.8$   
165  $\mu\text{g m}^{-3}$  (summer) in the same time period. Assuming direct proportionality between the contribution of HOA to total submicron  
166 organic mass increase and the increase of particle mass in each submode,  $0.9 \mu\text{g m}^{-3}$  (spring) and  $0.3 \mu\text{g m}^{-3}$  (summer) of  
167 particle mass were estimated as traffic-related organic components in the Aitken mode. Significant changes were also evident  
168 in the particle size metric (MMD), where a consistent decrease by 20-30% from about 170 nm (spring) or 160 nm (summer)  
169 to 130-140 nm (spring) or 120 nm (summer) was evident. This combined shift to smaller particle size and increase in total  
170 particle mass denotes a strong increase in the total number concentrations of particles in the Aitken mode range by at least a  
171 factor of 4-5 (assuming spherical particles and constant particle density) with significant additional contributions expected  
172 from elemental carbon particles and smaller Aitken mode and nucleation mode particles below the cut-off size (<50nm) of the  
173 AMS inlet lens.

174 Beyond 10:00, changes in submicron organic mass concentrations were dominated by variations in cooking-related organic  
175 aerosol (COA) components. During the main meal times (12:00 – 14:00 and 19:00 – 21:00) changes in organic submicron  
176 mass were almost entirely (>80%) caused by COA in both seasons (Table C1 in the Supporting Material) and daily maximum  
177 Aitken mode particle mass concentrations typically occur during these hours ( $5.5 - 6.2 \mu\text{g m}^{-3}$  in spring,  $3.1 - 3.5 \mu\text{g m}^{-3}$  in  
178 summer) with higher concentrations during the dinner period. Analogous to HOA, considering proportionality between COA  
179 fractional contribution and submode particle mass increase, primary cooking emissions accounted for  $1.7 - 1.8 \mu\text{g m}^{-3}$  of  
180 organic particle mass in the Aitken mode. Dinner in summer represents a notable exception, where the estimated cooking-  
181 related increase only amounted to  $0.5 \mu\text{g m}^{-3}$ . This is mainly due to specific local meteorological and geographical features  
182 owing to a greater frequency of easterly surface winds in the warmer season and the geographical distribution of cooking  
183 sources predominantly to the east of the sampling site (Sun et al., 2016; Lee et al., 2015), which led to considerably elevated  
184 Aitken mode mass concentration throughout the day including the late afternoon period and a correspondingly smaller  
185 additional increase during the dinner time. The aforementioned effect is particularly evident in the diurnal trend of the Aitken





186 mode particle mass fraction among total organic submicron mass (Figure 3b) which displayed a broad bell-shape during the  
187 day in summer with nominal increases of 9-10%, whereas in spring the variation follows a double peak behavior with nominal  
188 increases of 4-5% during the meal times which emphasize the more intermittent behavior of cooking-related particle  
189 contributions in spring. Cooking emissions had no conspicuous impact on particle size without notable trends in MMDs or the  
190 distribution width (GSDs) during the meal time periods (Figure 1a,b - *black lines in lower panels*).

191 In the accumulation mode, residual organic particle mass during the night hours (00:00 – 06:00) was 2.5 times larger in spring  
192 ( $5.5 \mu\text{g m}^{-3}$ ) than in summer ( $2.0 \mu\text{g m}^{-3}$ ). The mass concentration increase during the morning rush hour was larger in summer  
193 ( $\Delta M=3.9 \mu\text{g m}^{-3}$ ) than in spring ( $\Delta M=3.0 \mu\text{g m}^{-3}$ ), which was mainly caused by daytime increases of SOA components in  
194 summer (Lee et al., 2015), and consequently led to a lower fractional rush hour increase of traffic related organic constituents.  
195 Estimated particle mass contributions of traffic emissions in the accumulation mode amounted to  $1.8 \mu\text{g m}^{-3}$  in spring and  $1.6$   
196  $\mu\text{g m}^{-3}$  in summer. In terms of particle size, the onset of the rush hour had little conspicuous effects on the accumulation mode  
197 without clear trends in MMDs in both seasons. In summer the shift to smaller MMDs was accompanied by a notable narrowing  
198 of the Aitken mode, whereas in spring Aitken mode distribution widths remained largely stable throughout the day (Figure  
199 1a,b - *lower panels*).

200 Maximum accumulation mode particle concentrations during the meal hours reached  $10.5 - 12.3 \mu\text{g m}^{-3}$  in spring and  $6.0 -$   
201  $7.4 \mu\text{g m}^{-3}$  in summer. Analogous to the Aitken mode, estimated cooking-related particle contributions in the accumulation  
202 mode amounted to  $2.0 \mu\text{g m}^{-3}$  (spring) and  $1.0 \mu\text{g m}^{-3}$  (summer) during lunch, and to  $2.7 \mu\text{g m}^{-3}$  (spring) and  $2.4 \mu\text{g m}^{-3}$   
203 (summer) during dinner. Also, distribution widths (GSD) in the accumulation mode were not notably affected by cooking  
204 emissions. Seasonal differences were apparent in the mass median diameters of the accumulation mode. In spring, mode  
205 diameters remained largely constant ( $\pm 10\text{nm}$ ) apart from a subtle peak during the morning rush hour, indicative of minor  
206 condensational growth of traffic-related primary organics or rapidly formed secondary species. In summer, a consistent  
207 increase in particle size by  $20\text{nm}$  ( $\sim 5\%$ ) during the daytime points to particle growth through secondary formation as a  
208 governing factor.

209 Aitken mode particles contributed larger fractions to the total increase in organic submicron particle mass during the rush hour  
210 and mealtimes in spring (33-56%) than in summer (16-38%). These differences were presumably due to seasonal meteorology  
211 and associated effects on the formation, accumulation, and dispersion of particles from primary emission sources, as source  
212 strengths and characteristics of road traffic and commercial cooking are unlikely to vary with seasons in the inner-city urban  
213 areas of Hong Kong. Ambient temperatures and solar irradiation differed substantially with  $7^\circ\text{C}$  higher average temperatures  
214 (*measured at MK*) and three times higher integrated daily solar irradiation (*measured at HKUST*) in summer compared to  
215 spring (Figure D6e,f in the Supporting Material). Lower overall ambient temperatures enhance condensation and nucleation  
216 of gas-phase emissions and shift the gas-to-particle partitioning equilibrium of semi-volatile constituents towards the particle-  
217 phase. We expect these volatility effects to be a main contributing factor, as sampling took place in direct vicinity of the  
218 emission source, i.e. next to the road and thus potential impacts of physical effects such as enhanced near-ground mixing and  
219 dispersion through thermally induced convection in summer are expected to be of minor influence. Considering the previously



220 discussed estimated traffic contributions during the rush hour, the seasonal difference in mass concentration was much more  
221 pronounced in the Aitken mode (-67%,  $0.6 \mu\text{g m}^{-3}$ ) than the accumulation mode (-12%,  $0.2 \mu\text{g m}^{-3}$ ), consistent with the  
222 expected stronger impact of reduced nucleation and condensation of more volatile exhaust components on fresher, smaller  
223 particles in the warmer season.  
224 Comparing different size distribution sets (Figure D2 in the Supporting Material), the average concentration set in summer  
225 yielded notably larger resolved mass median diameters in both modes and greater Aitken mode mass compared to the median,  
226 25<sup>th</sup>, and 75<sup>th</sup> percentile concentration sets. This indicates a strong influence of extreme values (i.e. time periods with both  
227 larger particle size and larger particle mass concentrations) and thus greater variability in size distributions in the warmer  
228 season caused by specific high and low concentration events such as photochemical episodes and precipitation, evident in the  
229 greater relative span of organic mass concentrations in summer (See Table A2 in the Supporting Material: ratio of 10th and  
230 90th percentile to median concentration in NR-PM<sub>1</sub>). In spring such events masked the diurnal processes to a lesser extent and  
231 with consequently greater consistency across different size distribution sets.

### 232 233 Sulfate

234 Although variations of total submicron sulfate mass concentrations with time of day were generally subtle, distinct trends were  
235 notable in MMDs and integrated mode mass concentrations in both Aitken and accumulation mode.  
236 Generally, Aitken mode MMDs were 20% larger in spring (180nm) than in summer (150nm). While in spring fluctuations in  
237 Aitken mode MMDs were small throughout the day within a narrow range of +/- 10nm and without apparent regular features,  
238 the summertime diurnal variation exhibited a well-defined broad daytime peak with a shift to ~15nm larger particle diameters.  
239 A matching trend was evident in the accumulation mode where MMDs increased by ~20nm in summer. Conversely, in spring,  
240 a conspicuous nighttime peak in accumulation mode MMDs was observed in the low traffic period between 01:00 and 07:00  
241 which tracked closely with the diurnal variation of O<sub>3</sub> which peaked in the same period with the reduction of the NO<sub>x</sub> titration  
242 effects at low nighttime traffic volumes. While particulate sulfate production during the day can be achieved through both  
243 homogeneous gas-phase oxidation of SO<sub>2</sub> by the OH radical as well as heterogeneous oxidation of SO<sub>2</sub> by dissolved H<sub>2</sub>O<sub>2</sub> or  
244 O<sub>3</sub> (Seinfeld and Pandis, 2006), nighttime production is limited to the non-photochemical heterogeneous pathway. The  
245 apparent increase in accumulation mode particle size was also associated with an increase of integrated submode particle mass  
246 by ~0.7  $\mu\text{g/m}^3$  and thus points to heterogeneous SO<sub>2</sub> oxidation by residual ozone in the cooler and more humid spring season  
247 as a local source of particulate sulfate. In the warmer and drier summer season, no corresponding trend was apparent in either  
248 accumulation mode MMD or integrated mode concentration. The small magnitude of additionally produced sulfate (< 1  $\mu\text{g/m}^3$ )  
249 in spring renders the nighttime production a minor source of particulate sulfate however and affirms that the bulk of the  
250 accumulation mode sulfate burden at the urban roadside still originated from regional scale processes in both seasons. In  
251 summer, both modes exhibited notable increases in particle mass concentration levels during the daylight hours by ~80% in  
252 the Aitken mode and by ~35% in the accumulation mode compared to their respective nighttime “baseline“ concentrations.  
253 Integrated over the whole day, the additional sulfate burden above this baseline amounted to 0.4  $\mu\text{g/m}^3$  and 6  $\mu\text{g/m}^3$  and thereby





254 accounted for 34% and 11% of the total daily Aitken and accumulation mode particle mass respectively. This represents a  
255 rough estimation of possible local photochemical contributions to the Aitken and accumulation size mode in summer at the  
256 urban roadside, excluding possible physical effects, e.g. vertical mixing and advection or dilution laterally through the street  
257 canyon. Enhancements in particle mass by photochemical contributions were more pronounced in the Aitken mode, with the  
258 median fraction of Aitken mode particle mass among total AMS-measured particle mass (Figure 3) increasing substantially  
259 from its nighttime minimum at 4% to a maximum of 7% in the late afternoon in summer, while in spring the fraction remained  
260 almost constant at 6% throughout the day.

261 Considering different size distribution sets (Figure D2 in the Supporting Material), the 75<sup>th</sup> percentile size distributions and  
262 the average size distributions displayed notable increases in Aitken mode particle mass during the nighttime by 20-50% in  
263 spring. There was no corresponding trend in the accumulation mode, where changes in integrated mass concentration remained  
264 consistently <10%. The skewing of the average and higher percentile data indicates the influence of time periods with  
265 significantly elevated nighttime concentrations, likely related to events and atmospheric conditions conducive to the extensive  
266 formation of Aitken mode sulfate particles. The accumulation mode showed no notable changes in the average and 75<sup>th</sup>  
267 percentile data during the same time period, thus precluding physical processes such as transport or lowering of the planetary  
268 boundary layer as likely influential factors for these observations.

269

### 270 Nitrate

271 Particulate nitrate mass concentrations in the Aitken and accumulation mode exhibited similar diurnal variations in spring with  
272 lower daytime concentrations due to evaporation and higher nighttime concentrations where secondary formation and gas-to-  
273 particle partitioning prevailed. Analogous to sulfate, the Aitken mode MMDs for nitrate showed little change (<5%) throughout  
274 the day in both seasons. Aitken mode mass concentrations, however, exhibited a twofold increase over the dinner hours  
275 accounting for approximately  $0.9 \mu\text{g}/\text{m}^3$  (~16%) of additional particle nitrate mass per day. This may be due to the much higher  
276 abundance of small particles from cooking emissions providing additional surface area to facilitate gas-to-particle partitioning  
277 of nitrate. Increased signal intensities of oxygenated organic nitrogen ions (see Figure D7 in the Supporting Material) have  
278 also been observed during dinner suggesting that organic nitrate or other oxygenated nitrogen-containing organic species that  
279 produce nitrate fragments (Farmer et al., 2010) may too have contributed to this observed concentration peak. Accumulation  
280 mode nitrate mass increased by almost one-third in the low traffic period (01:00 – 07:00) compared to earlier night  
281 concentration levels (22:00 – 00:00) accompanied by a slight increase in MMD by ~10nm in spring. This signifies notable  
282 nighttime nitrate production through possibly nitric acid formation by ozone chemistry via the nitrate radical route under  
283 influence of organic components or formation of  $\text{N}_2\text{O}_5$  and subsequent hydrolysis during the night. Local nighttime nitrate  
284 production effectively contributed  $\sim 3 \mu\text{g}/\text{m}^3$  (~10%) to the total daily accumulation mode nitrate burden in spring.

285 Summertime nitrate production in Hong Kong has been mainly attributed to photochemical activity based on previous  
286 measurements of inorganic gas- and particle-phase nitrogen species at the suburban HKUST site (Griffith et al., 2015).  
287 Particulate nitrate mass concentrations at the urban Mong Kok site likewise exhibited clear daytime peaks, similar to sulfate



288 albeit at smaller magnitude with total integrated increases of  $\sim 0.3 \mu\text{g}/\text{m}^3$  and  $\sim 0.8 \mu\text{g}/\text{m}^3$  particulate nitrate per day in the  
289 Aitken and accumulation mode respectively. In the Aitken mode, particle mass remained elevated in the early night hours  
290 ( $\sim 19:00 - 22:00$ ), which was likely due to the previously mentioned cooking-related nitrate enhancement analogous to spring.  
291 The distribution of total submicron nitrate shifted slightly in favor of the Aitken mode in summer with  $\sim 18\%$  of total submicron  
292 nitrate found in the Aitken mode compared to  $\sim 14\%$  in spring.  
293 Comparing different size distribution sets (Figure D2 in the Supporting Material), the average size distributions displayed  
294 notable disparity compared to the remaining sets in both seasons. In summer, integrated particle mass concentrations and  
295 MMDs from the average set exhibited consistently larger values than those from the 25<sup>th</sup> percentile, 75<sup>th</sup> percentile, and median  
296 sets indicating significant influence of time periods with high nitrate concentrations and larger nitrate-containing particles. In  
297 spring, the average data exhibited a decrease in MMD in the Aitken mode from night to day, implying prolonged periods of  
298 significantly smaller daytime Aitken mode particles.  
299

### 300 3.2.1. Suburban coastal NR-PM<sub>1</sub>

301 The suburban HKUST site as a downwind receptor of urban and regional pollution was generally dominated by sulfate and  
302 oxygenated secondary organic aerosol (SOA) components and much lower fractions of primary organic constituents, which  
303 combined typically made up less than a quarter of total organics (Li et al., 2015).  
304

#### 305 Organics

306 There were significant seasonal differences with larger fractions (Figure 3a) and concentrations (Figure 4c) of Aitken mode  
307 mass in total organic submicron particle mass in spring and summer compared to fall and winter, indicating greater influence  
308 of closer-ranged formation sources in the warmer season. Springtime integrated Aitken mode mass concentrations ( $\sim 0.8 \mu\text{g}/\text{m}^3$ )  
309 were twice as high as those in winter ( $\sim 0.4 \mu\text{g}/\text{m}^3$ ). In the accumulation mode highest particle mass loadings were observed in  
310 fall ( $5 \mu\text{g}/\text{m}^3$ ) and lowest loadings in spring ( $3 \mu\text{g}/\text{m}^3$ ) following the frequency pattern of continental air mass influence (Figure  
311 D8 in the Supporting Material) in each season indicating continental transport of particulate mass or gas-phase precursors.  
312 Lowest mass concentrations in the Aitken mode typically occurred in the night hours (00:00 – 05:00) in a range of 0.3 – 0.5  
313  $\mu\text{g}/\text{m}^3$  in spring, summer, and winter, while in fall mass loadings of 0.7 - 0.8  $\mu\text{g}/\text{m}^3$  were reached. Diurnal changes were least  
314 pronounced in winter with largely constant integrated Aitken mode particle concentrations. In the remaining seasons, varying  
315 degrees of daytime changes were apparent with a general increase around 06:00, likely owing to citybound commuter traffic  
316 from surrounding roads to the west of the sampling site at 1-2km of lateral distance. This also led to a modest increase in  
317 particle polydispersity with a discernible widening of the Aitken mode size distributions (*black solid line, lowest panels in*  
318 *Figure 2*). Daily maxima in spring, summer and fall were reached in the early evening ( $\sim 21:00$ ) with marked differences in  
319 absolute mass concentrations depending on the respective season, from a summer time low of  $0.8 \mu\text{g}/\text{m}^3$  to a fall season high



320 of  $1.4 \mu\text{g}/\text{m}^3$ . Mass median diameters in the Aitken mode were smaller in the night hours and displayed subtle increments  
321 during the day in the range of 10-20 nm reaching their maximum typically in the late afternoon, with the exception of the fall  
322 season when mass median diameters displayed very little variation with time of day.

323 Total particle mass in the accumulation mode in spring and summer reached minima during the night hours ( $2 \mu\text{g}/\text{m}^3$ ) and  
324 maxima ( $3 \mu\text{g}/\text{m}^3$ ) around noon, remaining stable in the daylight hours thereafter. MMDs increased notably from 440nm at  
325 night to 510nm during the day in spring, while in summer a morning rise by  $\sim 30\text{nm}$  from 530nm to 560nm was obvious  
326 between 06:00 and 10:00 and coincided with the morning rush hour and the associated early morning peak of  $\text{NO}_x$  and an  
327 otherwise stable mode diameter of 530nm for the rest of the day. In fall, the increase in accumulation mode organic mass  
328 occurred much earlier, starting in the dark hours at 04:00, with a corresponding trend also evident for nitrate but absent for  
329 sulfate, indicating a common source of these organic and nitrate enriched particles. Nighttime MMDs for organics were  
330 generally larger (540nm) and decreased to a minimum of 510nm in the early afternoon accompanied by a slight widening of  
331 the distribution. In winter, mass concentrations decreased appreciably in the early morning hours and started to increase only  
332 beyond 10:00. In the colder seasons (fall, winter), a similar concentration pattern was also observed for gas-phase  $\text{SO}_2$  which  
333 is considered as a largely regional pollutant with few distinct local sources (Yuan et al., 2013), indicating that changes in  
334 boundary layer and mixing with regional background were likely the more dominant processes in winter.

335

### 336 Sulfate

337 Aitken mode sulfate mass concentrations peaked in the afternoon from spring throughout fall with maximum concentrations  
338 reached progressively later in the afternoon (14:00 in spring; 16:00 in fall). Nominal concentrations were highest in spring and  
339 summer ( $0.5\text{-}0.6 \mu\text{g}/\text{m}^3$ ), slightly lower in fall ( $0.4 \mu\text{g}/\text{m}^3$ ) and reached the lowest levels in winter ( $0.1 \mu\text{g}/\text{m}^3$ ). In addition to  
340 the afternoon peak, a conspicuous early morning peak of similar magnitude was evident in spring between 02:00 and 06:00. A  
341 greater proportion of southerly winds was evident in said time period compared to the overall seasonal wind frequency  
342 distribution (Figure D9a in the Supporting Material) and may indicate transport of sulfate from marine sources in the southern  
343 parts of Hong Kong. Diurnal variations in MMDs and GSDs were generally small and without obvious regular trends. Nominal  
344 mass median diameters were significantly lower in winter ( $\sim 170\text{nm}$ ) compared to spring and fall ( $\sim 190\text{nm}$ ) and summer  
345 ( $\sim 210\text{nm}$ ). Trends in accumulation mode particle mass were more pronounced. In spring, a shallow concentration valley during  
346 the late evening and night hours (20:00 to 03:00) with minimum concentrations of  $5 \mu\text{g}/\text{m}^3$  was apparent, while daytime  
347 concentrations stayed largely invariant at  $6 \mu\text{g}/\text{m}^3$ . The MMDs followed a similar variation with a minimum mode diameter  
348 around 550nm in the early hours of the day and slightly larger daytime MMDs around 570nm. Nominal concentrations were  
349 larger in summer with a nighttime valley concentration of  $7 \mu\text{g}/\text{m}^3$  and a well-pronounced broad day peak with a maximum of  
350  $9.5 \mu\text{g}/\text{m}^3$  in the early afternoon (14:00-15:00). A prior additional morning peak occurred between 04:00 and 10:00 with  
351 particle mass concentrations reaching  $8.5 \mu\text{g}/\text{m}^3$  related to a consistent north-easterly morning wind pattern (Figure D9b in the  
352 Supporting Material) and likely associated with transport from north-easterly coastal regions or nighttime fisheries related  
353 maritime traffic. The diurnal trend in mass median diameter was similar to that in spring with a night minimum of 570nm and



354 day maximum of 590nm. In fall, accumulation mode characteristics showed no significant diurnal variability, with a largely  
355 stable integrated particle mass of  $6 \mu\text{g}/\text{m}^3$  and only subtle MMD changes (585nm at night; 575nm during the day). In winter,  
356 two concentration dips with reductions by  $\sim 0.5 \mu\text{g}/\text{m}^3$  between 06:00 and 10:00 and between 18:00 and 22:00 were evident,  
357 while MMDs increased during the day between 10:00 and 15:00 from 520nm, peaking at a size of 540nm.

358

### 359 Nitrate

360 Nitrate particle mass in the Aitken mode was generally small from spring throughout fall amounting to  $0.01 - 0.06 \mu\text{g}/\text{m}^3$ .  
361 Winter time concentrations were larger in a range of  $0.06 - 0.08 \mu\text{g}/\text{m}^3$  during the day and  $0.10 - 0.12 \mu\text{g}/\text{m}^3$  in the late evening  
362 hours. The latter evening peak centered around 21:00 was evident in most seasons (except spring) and accounted for 12-23%  
363 ( $0.1-0.25 \mu\text{g}/\text{m}^3$ ) of total daily Aitken mode nitrate mass burden. Similar to the urban roadside location, these nighttime nitrate  
364 peaks coincided with the peak period of organic cooking aerosol concentrations (Figure D10 in the Supporting Material),  
365 which were however significantly smaller at the suburban measurement site and mainly attributed to the operation of an on-  
366 campus student canteen (Li et al., 2015). Trends in mass median diameters varied between seasons with no discernible trend  
367 in winter, a subtle decreasing trend with time of day in spring and broad daytime diameter increases in summer and fall. Solar  
368 irradiation in these two seasons was comparatively high (Figure D6b,c in the Supporting Material) indicating that  
369 photochemical nitrate production in the Aitken mode may have led to this observed growth in particle size.

370 Integrated particle mass concentrations in the accumulation mode only exhibited subtle variations from spring throughout fall,  
371 with essentially constant diurnal concentrations in spring, a subtle daytime peak in summer which accounted for  $\sim 15\%$  of total  
372 daily accumulation mode nitrate (corresponding to  $0.7 \mu\text{g}/\text{m}^3$ ) and a conspicuous morning peak between 04:00 and 10:00 in  
373 fall accounting for  $\sim 5\%$  of total daily accumulation mode nitrate (corresponding to  $0.5 \mu\text{g}/\text{m}^3$ ). Clearer seasonal differences  
374 were evident in the trends of MMDs. In spring, MMDs decreased appreciably over the late evening hours (21:00-0:00) with a  
375 concurrent widening of the size distribution (increase in GSD). In summer, accumulation mode diameters decreased during  
376 the day by  $\sim 40\text{nm}$  with a similar trend in accumulation mode organics. Winter time MMDs exhibited a more complex pattern  
377 with larger mode diameters in the early hours (04:00 – 10:00) and during the noon-time, and a late-afternoon dip leading to  
378 larger spread of intra-day mode diameters ranging from 510nm to 570nm.

379 In comparison to the urban roadside measurements, diurnal particle size characteristics and mass concentrations in the Aitken  
380 and accumulation mode were much more variable for all investigated species at the suburban HKUST site, indicating that  
381 longer time scale processes and irregular events (transport patterns, local meteorology) were probably more important in  
382 governing particle size distribution characteristics than diurnal processes.

### 383 **3.3. Day-to-day size distributions**

384 To evaluate the evolution of particle size distributions within seasons, average species-specific size distributions were  
385 generated by averaging raw distributions over 24h periods (between 0:00 and 23:59). There was clear long-term variability in



386 both resolved Aitken and accumulation mode MMDs and integrated submode particle mass concentrations for all species  
387 (Figure D11 in the Supporting Material) and overall seasonal differences which have been briefly addressed in the discussion  
388 of the diurnal size distribution variations between seasons. Figure 4 depicts the overall average values for all daily fitted MMDs  
389 and integrated particle mass concentrations in both the Aitken and accumulation mode at the suburban HKUST and urban MK  
390 sites.

### 391 3.3.1. Seasonal trends

392 For the MK roadside station, particle mode diameters were generally larger in spring than in summer for all three investigated  
393 species, but with clear differences in the magnitude of changes among individual species. In the Aitken mode, organics and  
394 sulfate displayed a moderate decrease in mode diameter by 7-8% each, while nitrate saw a more significant decrease by 25%  
395 from spring to summer. In contrast, accumulation mode MMDs for organics exhibited only a subtle decrease by 5% and more  
396 substantial decreases for sulfate and nitrate by 20-22% each. Total Aitken mode particle mass decreases varied strongly: -15%  
397 for organics, -36% for sulfate and -67% for nitrate. In the accumulation mode, organics and sulfate exhibited similar relative  
398 decreases by 40-46%, while nitrate particle mass reduced drastically by 85%.

399 At the suburban HKUST site, Aitken mode MMDs of nitrate and organics decreased with the progression of seasons from  
400 spring to winter with highest mode diameters observed in spring and summer and appreciable decreases in winter by -9% for  
401 nitrate and -25% for organics compared to the warmer seasons. Sulfate displayed a similar winter time decrease in MMD (-  
402 15%) and an increase of similar magnitude in the summer season (+13%) compared to spring and fall. Variations in sulfate  
403 and organic accumulation mode diameters were minor between spring and fall, while wintertime MMDs were 7-12% lower.  
404 Nitrate exhibited an overall higher variability in mass median diameters in the accumulation mode in spring (larger standard  
405 deviation) and with on average 10% lower MMDs compared to other seasons. In line with the reduction in Aitken mode MMDs  
406 in winter, the integrated Aitken mode particle mass decreased as well, by -16% for organics and almost -75% for sulfate,  
407 whereas nitrate contributions remained largely stable throughout the seasons. Organic accumulation mode particle mass was  
408 significantly higher in the fall and winter season by factors of 1.6 – 2. Diurnal variations in the degree of oxygenation were  
409 least pronounced in these seasons (Li et al., 2015) suggesting that influence of transport in autumn and winter likely dominated  
410 over local formation, thus exerting greater effects on particle mass in the larger size mode. Particulate nitrate concentrations  
411 were generally low in the accumulation mode from spring through fall, but increased sharply in winter by factors of 3 – 4.  
412 Sulfate accumulation mode mass concentrations remained more stable but saw significant summer time enhancements by  
413 ~30% likely due to photochemical activity which also led to high concentrations of Ox and a higher degree of oxygenation of  
414 organic aerosol among the four seasons (Li et al., 2015).

415 Large particles contribute more to particle volume and hence particle mass. Correspondingly, the total submicron concentration  
416 of a given species is typically governed by changes in the accumulation mode particle mass and accordingly observed  
417 correlation values between integrated accumulation mode particle mass and individual NR-PM<sub>1</sub> species mass concentrations



418 were generally high ( $R_{pr} > 0.90$ ) at both measurement sites (Figure D12 in the Supporting Material). This applied to both  
419 measurement sites regardless of the season. Aitken mode trends were less akin. At the urban roadside station, neither sulfate  
420 nor nitrate particle mass in the Aitken mode notably correlated with the respective total submicron species mass concentration  
421 in spring (all  $R_{pr} \leq 0.20$ ), whereas in summer correlations were more significant with  $R_{pr} = 0.51$  for sulfate and  $R_{pr} = 0.80$  for  
422 nitrate. This signifies that periods of greater species mass concentrations were more likely to be caused by increases in both  
423 Aitken and accumulation mode particle mass indicating that particle formation and growth affecting smaller particles was more  
424 likely to occur in the warmer season. For organics, Aitken mode particle mass and submicron species mass correlated only  
425 weakly ( $R_{pr} = 0.26$  in spring and  $R_{pr} = 0.38$  in summer), i.e. each organic particle submode was governed by largely different  
426 dominant sources or formation processes in both seasons at the roadside.

427 At the suburban background site, Aitken mode particle mass for sulfate showed little correlation with total submicron sulfate  
428 concentration ( $R_{pr} \leq 0.10$ ) with the exception of the spring season ( $R_{pr} = 0.36$ ) where more frequent wet and foggy conditions  
429 may have facilitated sulfate formation in both size modes. For organics and nitrate significantly larger correlation coefficients  
430 of submode particle mass to total species concentration ( $0.5 \leq R_{pr} \leq 0.7$ ) were observed in most seasons (spring, summer,  
431 winter) indicating significant influence of local or regional formation processes on organic and nitrate Aitken mode particulate  
432 mass at the suburban receptor location. In the fall season, much weaker correlations ( $0.2 \leq R_{pr} \leq 0.4$ ) were likely caused by the  
433 dominance of continental air mass influence (Figure S8c in the Supporting Material) and greater influence of aged  
434 accumulation mode particles on total submicron nitrate mass concentrations.

### 435 3.3.2. Inferred changes in mixing state

436 Shifts in mixing state of ambient particles can be inferred from the inter-species analysis of mass median diameters. Close  
437 nominal agreement (i.e. diameter ratios close to 1) infer that particles containing different species were similar in size which  
438 thus most likely represents a largely internally mixed particle population, while the spread of data (correlation coefficient)  
439 indicates the temporal homogeneity or divergence of resolved mode diameters. A hypothetically perfectly internally mixed  
440 particle population over the whole sampling period would, therefore, yield MMD ratios and Pearson's R values of 1 between  
441 species, while larger or smaller values are indicative of a greater frequency of heterogeneous (i.e. more externally mixed)  
442 particle populations (Figure 5).

443 At the urban Mong Kok site, changes in accumulation mode mass median diameters for nitrate and sulfate followed similar  
444 trends ( $R_{pr} = 0.88-0.89$ ) and with diameter ratios close to 1 (0.94–0.95). Similarly, fitted accumulation mode diameters of  
445 organic constituents predominantly followed that of sulfate in spring nominally (diameter ratio 0.88) and temporally ( $R_{pr} =$   
446 0.80). The nominal agreement of organic and sulfate accumulation mode diameters persisted (diameter ratio 1.03) overall in  
447 summer, however, there was significantly more temporal divergence ( $R_{pr} = 0.65$ ) indicating a greater frequency of time periods  
448 with external mixing of particle populations comprising different fractions of organic constituents.





449 External mixing is more prevalent for freshly formed smaller particles which have typically undergone less condensational  
450 growth and coagulation. Indeed, the correlation coefficients of both nitrate and organic Aitken mode MMDs with respect to  
451 sulfate were notably lower (0.50 and 0.62) indicating frequent periods of particle populations with different species prevailing  
452 in different size regions within the Aitken mode. Sulfate and nitrate were still more likely to occur internally mixed in the  
453 Aitken mode in spring with similar diameters (nitrate to sulfate MMD ratio = 1.00), while organic Aitken mode MMDs were  
454 consistently lower, indicating greater fractions of organic dominated particles towards the lower end and more inorganic  
455 dominated particles towards the upper end of the fitted Aitken mode. In summer, both nitrate and organic MMDs tended to be  
456 lower than those of sulfate (diameter ratios of 0.79 – 0.83) but similar to each other, thus implying a shift to externally mixed  
457 populations of more nitrate and organic enhanced and internally mixed smaller Aitken mode particles and sulfate dominated  
458 larger Aitken mode particles.

459 At the suburban HKUST site, accumulation mode MMDs of both nitrate and organics were generally quite similar to those of  
460 sulfate with diameter ratios of 0.88 – 1.06. Compared to the urban site, correlation coefficients of nitrate and sulfate were  
461 consistently lower (0.54 – 0.67) indicating a much greater frequency of time periods where sulfate and nitrate dominated  
462 particles in the accumulation exhibited significantly different particle size distributions. In winter, organic MMDs were  
463 consistently lower than those of sulfate and nitrate indicating a greater proportion of externally mixed particle populations with  
464 organics enriched particles in the lower accumulation size range and inorganic dominated particles in the larger accumulation  
465 size range. The least variability in particle size was observed in the summer season where MMDs in both Aitken and  
466 accumulation mode displayed variations in relatively narrow ranges between 200-250nm and 500-700nm, whereas in the  
467 remaining seasons time periods with particle populations of lower MMD were more frequent, extending to MMDs as low as  
468 100nm in the Aitken mode and 300nm in the accumulation mode. In the Aitken mode, mass median diameters overall were  
469 quite similar across species, with diameter ratios of organic and nitrate distributions to those of sulfate in the range of 0.87 –  
470 1.06, indicating that they generally covered a similar size range. The temporal agreement was highly variable with correlation  
471 coefficients ( $R_{pr}$ ) spanning from 0.21 to 0.75 indicating that Aitken mode particle populations at the suburban site were  
472 generally more diverse and likely influenced by a greater range of particle formation and growth mechanisms compared to the  
473 urban Mong Kok site.



#### 474 4. Conclusion

475 A detailed analysis of AMS mass-based particle size distributions of sulfate, nitrate, and organics in submicron particulate  
476 matter measured at two contrasting locations in Hong Kong during two field campaigns has been undertaken. Deconvolution  
477 of size distributions into Aitken and accumulation submodes was accomplished by log-normal peak fitting and trends in particle  
478 size (mass median diameters), dispersity (geometric standard deviation) and overall particle mass (integrated mode area) were  
479 discussed on a diurnal time scale and on a daily basis to evaluate longer-term changes in size distribution characteristics. At  
480 the urban roadside location, clear diurnal influences of primary particle and gas-phase species were evident affecting both  
481 inorganic and organic component size distributions. Traffic and cooking contributed an estimated  $0.3 - 0.9 \mu\text{g m}^{-3}$  and  $0.5 -$   
482  $1.8 \mu\text{g m}^{-3}$  of organic component particle mass in the Aitken mode, and  $1.6 - 1.8 \mu\text{g m}^{-3}$  and  $1.0 - 2.7 \mu\text{g m}^{-3}$  respectively in  
483 the accumulation mode with concentrations level varying with seasons. Notable changes in Aitken mode mass median  
484 diameters of organics were limited to the morning rush hour. Daytime particle concentration maxima of sulfate and nitrate in  
485 summer indicated substantial influence of photochemical processes, which also led to increments in mass median diameters in  
486 the accumulation mode thus inferring associated particle growth. Nocturnal nitrate formation was apparent in the accumulation  
487 mode in spring concurring with the nighttime peak of ozone at the roadside, while in the Aitken mode nitrate particle  
488 concentrations were significantly elevated during the dinner hours. Organics-related size distributions were mostly governed  
489 by intra-day changes at the urban site with very similar trends across different size distribution sets (i.e. concentration regimes),  
490 while disparities in diurnal variations among different size distribution sets were evident for nitrate and sulfate, particularly  
491 affecting the average sets, indicating stronger influence of irregular external factors which were not associated with diurnal  
492 time scale processes.

493 Suburban particle size distributions exhibited variable diurnal characteristics, suggesting that irregular processes such as  
494 transport and seasonal meteorological conditions were the more dominant processes influencing particle size characteristics.  
495 Aitken mode particle mass of organics was significantly larger in spring and summer indicating greater influence of more local  
496 formation sources in the warm season. In the accumulation mode, organic particle mass concentrations were highest in fall and  
497 lowest in spring, following the frequency pattern of continental air mass influence. For sulfate, Aitken mode mass  
498 concentrations mass concentrations peaked in the afternoon from spring throughout fall with highest nominal concentrations  
499 in spring and summer and lowest levels in winter, while accumulation mode particle mass was highest in summer and fall and  
500 lowest in winter, similar to the trend observed among organic constituents.

501 Nitrate particle mass in the Aitken mode was generally small in most seasons ( $0.01 - 0.06 \mu\text{g m}^{-3}$ ), except winter where daytime  
502 concentrations reached  $\sim 0.1 \mu\text{g m}^{-3}$ . In both modes, changes in mass median diameters varied temporally and in magnitude  
503 with seasons, indicating a stronger influence of specific meteorological conditions on the properties of nitrate-containing  
504 particles at the suburban site. At the urban site, periods of greater inorganic species mass concentrations were more likely to  
505 be caused by increases in both Aitken and accumulation mode particle mass in summer, indicating that particle formation and  
506 growth affecting smaller particles was more likely to occur in the warmer season. At the suburban receptor location, significant



507 correlation of submode particle mass to total species concentration ( $0.5 \leq R_{pr} \leq 0.7$ ) was observed for organics and nitrate in  
508 most seasons (spring, summer, winter) suggesting notable influence of local or regional formation processes on organic and  
509 nitrate Aitken mode particulate mass. Variations in particle mixing state were examined by evaluation of inter-species mass  
510 median diameter trends at both measurement sites. In the accumulation mode at the urban site, internal mixing appeared to be  
511 prevalent in spring, while greater frequency of time periods with external mixing of particle populations comprising different  
512 fractions of organic constituents was observed in summer. External mixing was predominant in the Aitken mode at the urban  
513 location in both seasons. At the suburban site, sulfate and nitrate in the accumulation mode more frequently exhibited differing  
514 particle size distributions in all seasons signifying a greater extent of external mixing. In winter, external mixing of more  
515 organics enriched particles in the lower accumulation size range was evident.

## 516 Acknowledgements

517 This work was supported by the Environmental Conservation Fund of Hong Kong (project number ECWW09EG04). Chak K.  
518 Chan gratefully acknowledges the startup fund of the City University of Hong Kong.

## 519 References

- 520 Abbatt, J. P. D., Broekhuizen, K., and Pradeep Kumar, P.: Cloud condensation nucleus activity of internally mixed  
521 ammonium sulfate/organic acid aerosol particles, *Atmospheric Environment*, 39, 4767-4778,  
522 10.1016/j.atmosenv.2005.04.029, 2005.
- 523 Aiken, A. C., et al.: Mexico City aerosol analysis during MILAGRO using high resolution aerosol mass spectrometry at the  
524 urban supersite (T0) - Part 1: Fine particle composition and organic source apportionment, *Atmospheric Chemistry and*  
525 *Physics*, 9, 6633-6653, 2009.
- 526 Bahreini, R., et al.: Design and Operation of a Pressure-Controlled Inlet for Airborne Sampling with an Aerodynamic  
527 Aerosol Lens, *Aerosol Science and Technology*, 42, 465-471, 10.1080/02786820802178514, 2008.
- 528 Bian, Q., Huang, X. H. H., and Yu, J. Z.: One-year observations of size distribution characteristics of major aerosol  
529 constituents at a coastal receptor site in Hong Kong &ndash; Part 1: Inorganic ions and oxalate, *Atmos. Chem. Phys.*, 14,  
530 9013-9027, 10.5194/acp-14-9013-2014, 2014.
- 531 Canagaratna, M. R., et al.: Chemical and microphysical characterization of ambient aerosols with the aerodyne aerosol mass  
532 spectrometer, *Mass Spectrometry Reviews*, 26, 185-222, 10.1002/mas.20115, 2007.
- 533 Cheung, K., et al.: Characterization and source identification of sub-micron particles at the HKUST Supersite in Hong Kong,  
534 *Science of The Total Environment*, 527-528, 287-296, <http://dx.doi.org/10.1016/j.scitotenv.2015.04.087>, 2015.
- 535 Crippa, M., et al.: Wintertime aerosol chemical composition and source apportionment of the organic fraction in the  
536 metropolitan area of Paris, *Atmos. Chem. Phys.*, 13, 961-981, 10.5194/acp-13-961-2013, 2013.



- 537 DeCarlo, P. F., Slowik, J. G., Worsnop, D. R., Davidovits, P., and Jimenez, J. L.: Particle morphology and density  
538 characterization by combined mobility and aerodynamic diameter measurements. Part 1: Theory, *Aerosol Science and*  
539 *Technology*, 38, 1185-1205, 10.1080/027868290903907, 2004.
- 540 Docherty, K. S., et al.: The 2005 Study of Organic Aerosols at Riverside (SOAR-1): instrumental intercomparisons and fine  
541 particle composition, *Atmospheric Chemistry and Physics*, 11, 12387-12420, 10.5194/acp-11-12387-2011, 2011.
- 542 Farmer, D. K., et al.: Response of an aerosol mass spectrometer to organonitrates and organosulfates and implications for  
543 atmospheric chemistry, *Proceedings of the National Academy of Sciences of the United States of America*, 107, 6670-6675,  
544 10.1073/pnas.0912340107, 2010.
- 545 Griffith, S. M., Huang, X. H. H., Louie, P. K. K., and Yu, J. Z.: Characterizing the thermodynamic and chemical  
546 composition factors controlling PM<sub>2.5</sub> nitrate: Insights gained from two years of online measurements in Hong Kong,  
547 *Atmospheric Environment*, 122, 864-875, <http://dx.doi.org/10.1016/j.atmosenv.2015.02.009>, 2015.
- 548 Huang, X. F., et al.: Characterization of submicron aerosols at a rural site in Pearl River Delta of China using an Aerodyne  
549 High-Resolution Aerosol Mass Spectrometer, *Atmospheric Chemistry and Physics*, 11, 1865-1877, 10.5194/acp-11-1865-  
550 2011, 2011.
- 551 Huang, X. H. H., Bian, Q. J., Ng, W. M., Louie, P. K. K., and Yu, J. Z.: Characterization of PM<sub>2.5</sub> Major Components and  
552 Source Investigation in Suburban Hong Kong: A One Year Monitoring Study, *Aerosol and Air Quality Research* 14, 237-  
553 250, 2014.
- 554 John, W.: Size Distribution Characteristics of Aerosols, in: *Aerosol Measurement*, John Wiley & Sons, Inc., 41-54, 2011.
- 555 Kerminen, V. M., et al.: Cloud condensation nuclei production associated with atmospheric nucleation: a synthesis based on  
556 existing literature and new results, *Atmos. Chem. Phys.*, 12, 12037-12059, 10.5194/acp-12-12037-2012, 2012.
- 557 Köhler, H.: The nucleus in and the growth of hygroscopic droplets, *Transactions of the Faraday Society*, 32, 1152-1161,  
558 10.1039/tf9363201152, 1936.
- 559 Lee, B. P., Li, Y. J., Yu, J. Z., Louie, P. K. K., and Chan, C. K.: Physical and chemical characterization of ambient aerosol  
560 by HR-ToF-AMS at a suburban site in Hong Kong during springtime 2011, *Journal of Geophysical Research: Atmospheres*,  
561 118, 8625-8639, 10.1002/jgrd.50658, 2013.
- 562 Lee, B. P., Li, Y. J., Yu, J. Z., Louie, P. K. K., and Chan, C. K.: Characteristics of submicron particulate matter at the urban  
563 roadside in downtown Hong Kong—Overview of 4 months of continuous high-resolution aerosol mass spectrometer  
564 measurements, *Journal of Geophysical Research: Atmospheres*, 120, 7040-7058, 10.1002/2015JD023311, 2015.
- 565 Li, Y. J., Lee, B. Y. L., Yu, J. Z., Ng, N. L., and Chan, C. K.: Evaluating the degree of oxygenation of organic aerosol during  
566 foggy and hazy days in Hong Kong using high-resolution time-of-flight aerosol mass spectrometry (HR-ToF-AMS), *Atmos.*  
567 *Chem. Phys.*, 13, 8739-8753, 10.5194/acp-13-8739-2013, 2013.
- 568 Li, Y. J., Lee, B. P., Su, L., Fung, J. C. H., and Chan, C. K.: Seasonal characteristics of fine particulate matter (PM) based on  
569 high resolution time-of-flight aerosol mass spectrometric (HR-ToF-AMS) measurements at the HKUST Supersite in Hong  
570 Kong, *Atmos. Chem. Phys.*, 15, 37-53, doi:10.5194/acp-15-37-2015, 2015.

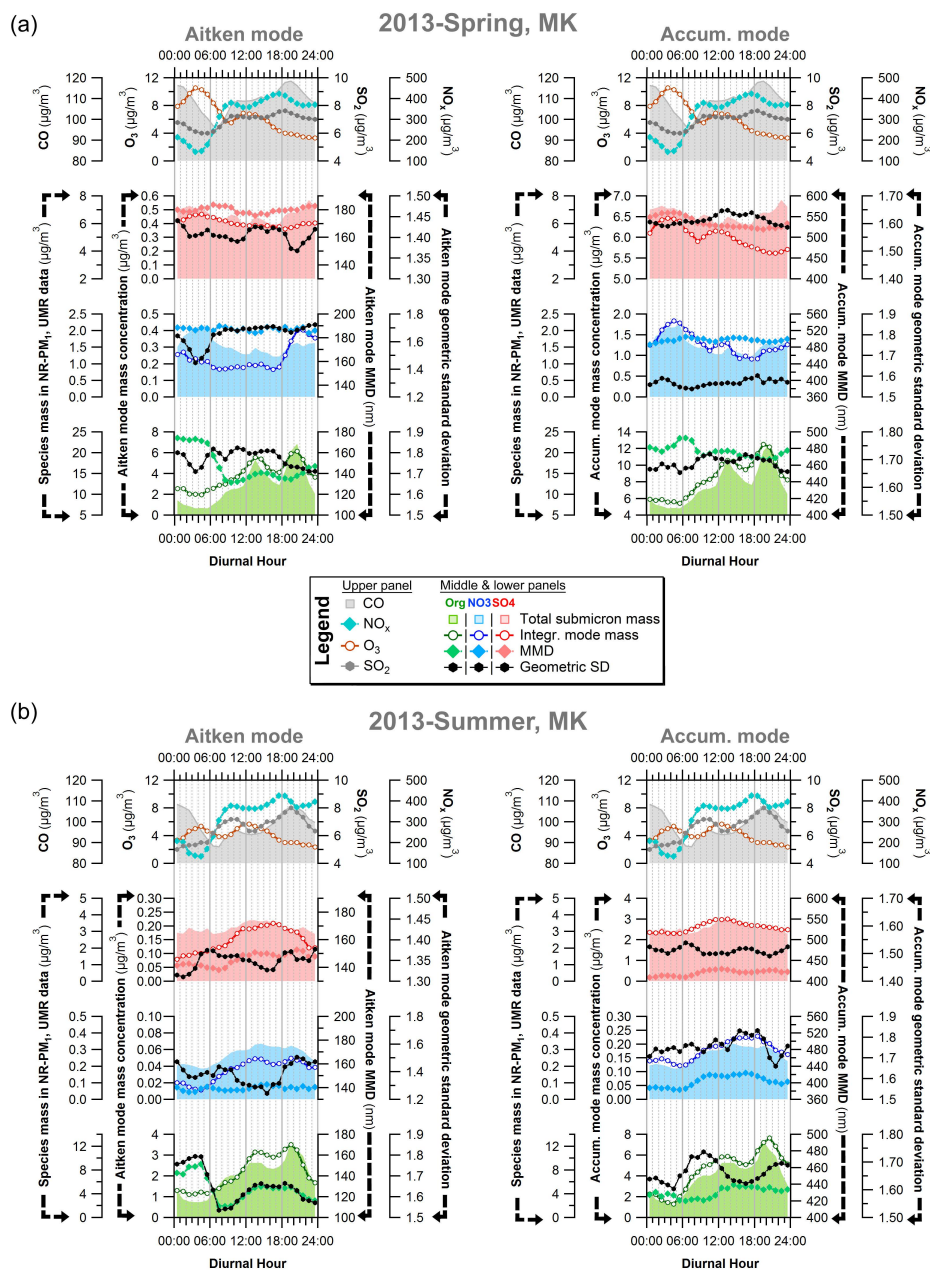


- 571 Liu, P. S. K., et al.: Transmission efficiency of an aerodynamic focusing lens system: Comparison of model calculations and  
572 laboratory measurements for the Aerodyne Aerosol Mass Spectrometer, *Aerosol Science and Technology*, 41, 721-733,  
573 10.1080/02786820701422278, 2007.
- 574 Man, H., et al.: Comparison of Daytime and Nighttime New Particle Growth at the HKUST Supersite in Hong Kong,  
575 *Environmental Science & Technology*, 49, 7170-7178, 10.1021/acs.est.5b02143, 2015.
- 576 Meng, J. W., Yeung, M. C., Li, Y. J., Lee, B. Y. L., and Chan, C. K.: Size-resolved cloud condensation nuclei (CCN)  
577 activity and closure analysis at the HKUST Supersite in Hong Kong, *Atmos. Chem. Phys.*, 14, 10267-10282, 10.5194/acp-  
578 14-10267-2014, 2014.
- 579 Mohr, C., et al.: Identification and quantification of organic aerosol from cooking and other sources in Barcelona using  
580 aerosol mass spectrometer data, *Atmos. Chem. Phys.*, 12, 1649-1665, 10.5194/acp-12-1649-2012, 2012.
- 581 Slowik, J. G., et al.: Particle morphology and density characterization by combined mobility and aerodynamic diameter  
582 measurements. Part 2: Application to combustion-generated soot aerosols as a function of fuel equivalence ratio, *Aerosol  
583 Science and Technology*, 38, 1206-1222, 10.1080/027868290903916, 2004.
- 584 Sun, C., et al.: Continuous measurements at the urban roadside in an Asian megacity by Aerosol Chemical Speciation  
585 Monitor (ACSM): particulate matter characteristics during fall and winter seasons in Hong Kong, *Atmos. Chem. Phys.*, 16,  
586 1713-1728, 10.5194/acp-16-1713-2016, 2016.
- 587 Sun, Y. L., et al.: Characterization of the sources and processes of organic and inorganic aerosols in New York city with a  
588 high-resolution time-of-flight aerosol mass spectrometer, *Atmospheric Chemistry and Physics*, 11, 1581-1602, 10.5194/acp-  
589 11-1581-2011, 2011.
- 590 Takegawa, N., et al.: Performance of an Aerodyne Aerosol Mass Spectrometer (AMS) during Intensive Campaigns in China  
591 in the Summer of 2006, *Aerosol Science and Technology*, 43, 189-204, 10.1080/02786820802582251, 2009.
- 592 Westervelt, D. M., et al.: Formation and growth of nucleated particles into cloud condensation nuclei: model-measurement  
593 comparison, *Atmos. Chem. Phys.*, 13, 7645-7663, 10.5194/acp-13-7645-2013, 2013.
- 594 Yao, X., Lau, N. T., Chan, C. K., and Fang, M.: Size distributions and condensation growth of submicron particles in on-  
595 road vehicle plumes in Hong Kong, *Atmospheric Environment*, 41, 3328-3338, 10.1016/j.atmosenv.2006.12.044, 2007a.
- 596 Yao, X., Ling, T. Y., Fang, M., and Chan, C. K.: Size dependence of in situ pH in submicron atmospheric particles in Hong  
597 Kong, *Atmospheric Environment*, 41, 382-393, 10.1016/j.atmosenv.2006.07.037, 2007b.
- 598 Yuan, Z., Yadav, V., Turner, J. R., Louie, P. K. K., and Lau, A. K. H.: Long-term trends of ambient particulate matter  
599 emission source contributions and the accountability of control strategies in Hong Kong over 1998–2008, *Atmospheric  
600 Environment*, 76, 21-31, <http://dx.doi.org/10.1016/j.atmosenv.2012.09.026>, 2013.
- 601 Zhang, J. K., et al.: Characterization of submicron aerosols during a month of serious pollution in Beijing, 2013, *Atmos.  
602 Chem. Phys.*, 14, 2887-2903, 10.5194/acp-14-2887-2014, 2014.
- 603 Zhang, Q., et al.: Insights into the chemistry of new particle formation and growth events in Pittsburgh based on aerosol  
604 mass spectrometry, *Environmental Science & Technology*, 38, 4797-4809, 10.1021/es035417u, 2004.



- 605 Zhang, Q., Canagaratna, M. R., Jayne, J. T., Worsnop, D. R., and Jimenez, J. L.: Time- and size-resolved chemical  
606 composition of submicron particles in Pittsburgh: Implications for aerosol sources and processes, *Journal of Geophysical*  
607 *Research-Atmospheres*, 110, D07s09 Artn d07s09, 2005.
- 608 Zheng, M., Kester, D. R., Wang, F., Shi, X., and Guo, Z.: Size distribution of organic and inorganic species in Hong Kong  
609 aerosols during the wet and dry seasons, *J. Geophys. Res.*, 113, D16303, 10.1029/2007jd009494, 2008.
- 610 Zhuang, H., Chan, C. K., Fang, M., and Wexler, A. S.: Size distributions of particulate sulfate, nitrate, and ammonium at a  
611 coastal site in Hong Kong, *Atmospheric Environment*, 33, 843-853, 10.1016/s1352-2310(98)00305-7, 1999.





612

613

**Figure 1.** Mode diameter (mass median diameter - MMD, *light colored line and solid marker*), integrated mode mass concentration (*dark colored line and opaque marker*) and width (geometric standard deviation, *black line and black marker*) of the Aitken mode and accumulation mass mode from diurnal peak fits bimodal of size distributions at the urban Mong Kok site and V-mode AMS species concentrations (*shaded background*) for organics, nitrate and sulfate (*bottom to top*) in (a) Spring 2013 and (b) Summer 2013; The top panel depicts the diurnal variations of relevant gas-phase pollutants ( $\text{O}_3$ , CO,  $\text{NO}_x$ ,  $\text{SO}_2$ ) measured at the adjacent Mong Kok Air Quality Monitoring Site (MK AQMS); identical plots over each mode

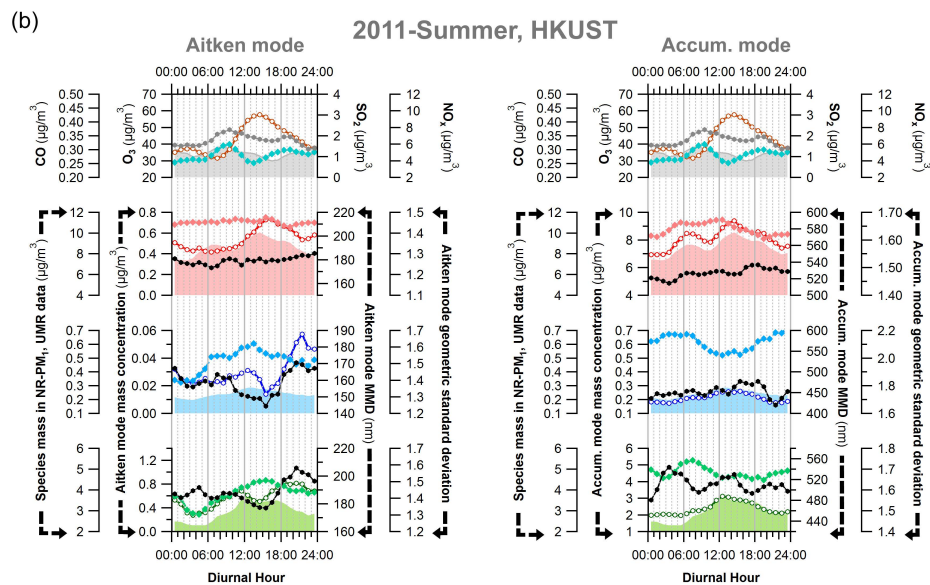
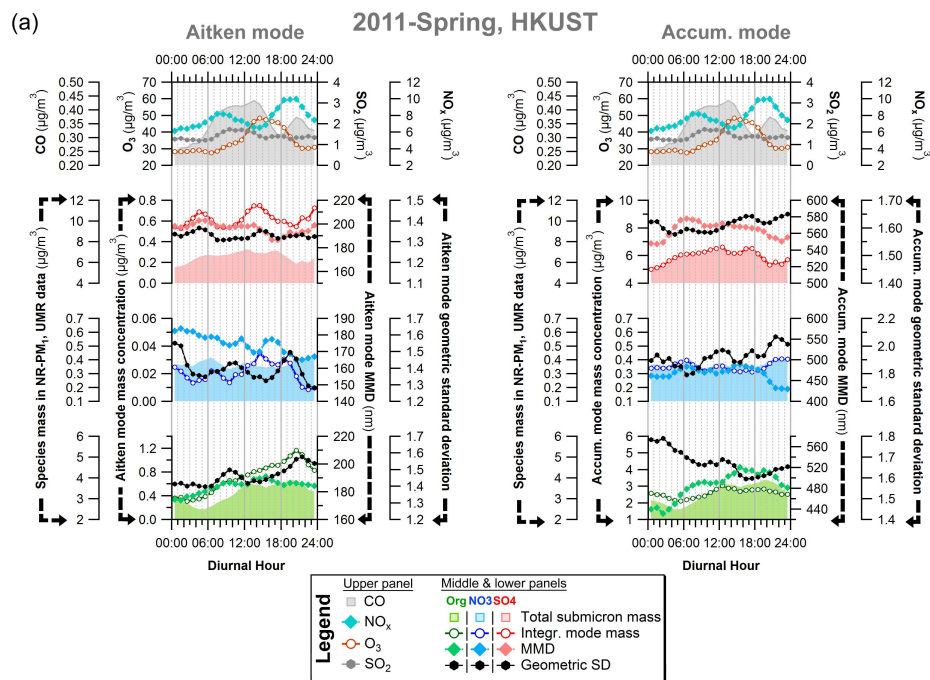
614

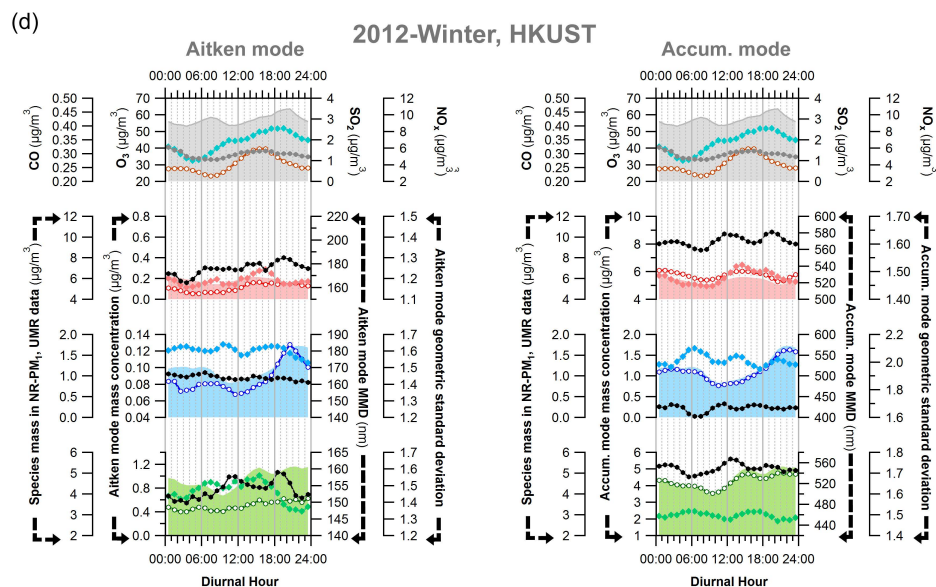
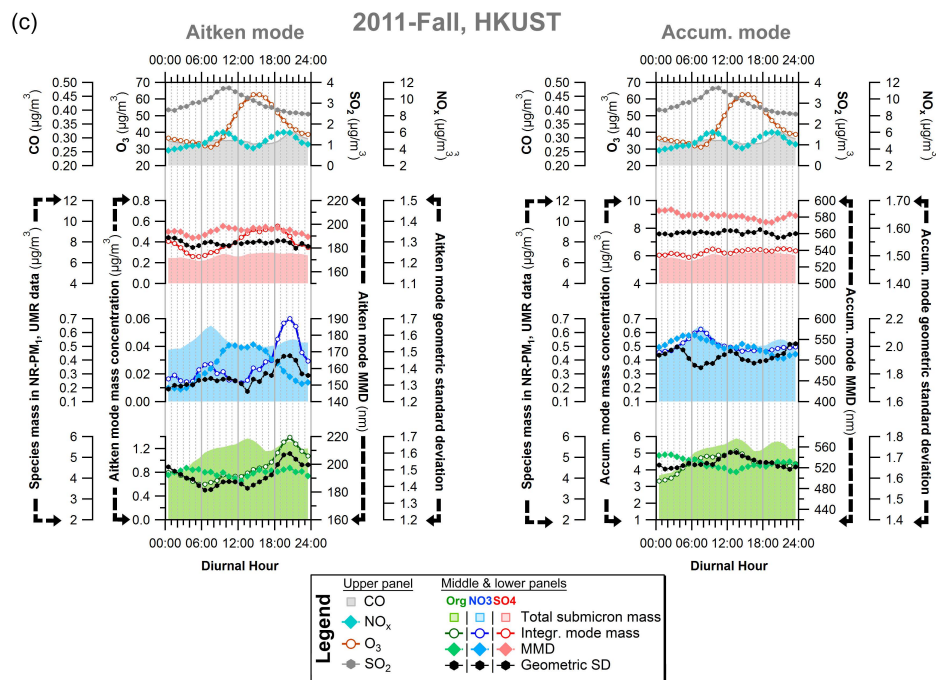
615

616

617

618

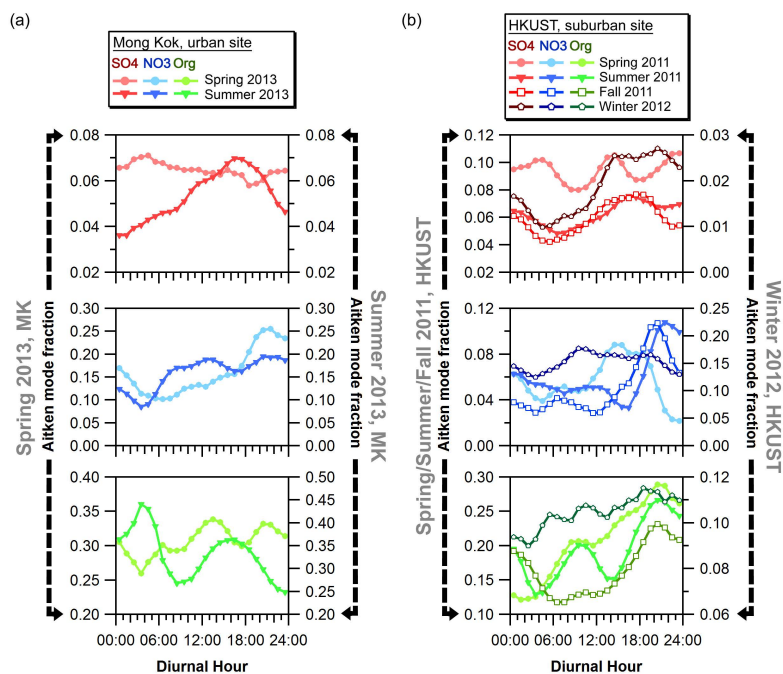




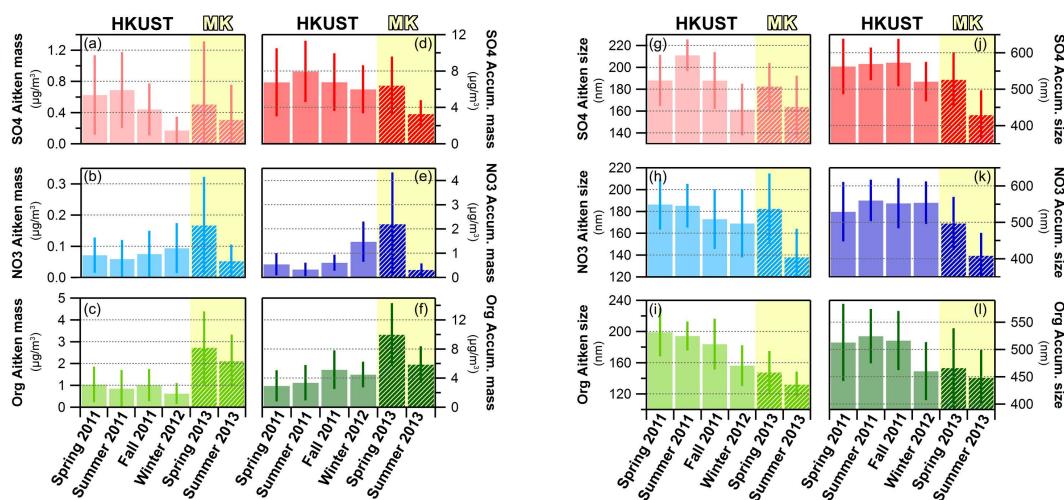
620

621 **Figure 2.** Mode diameter (mass median diameter - MMD, *light colored line and solid marker*), integrated mode mass concentration (*dark*  
 622 *colored line and opaque marker*) and width (geometric standard deviation, *black line and black marker*) of the Aitken mode and  
 623 accumulation mode from bimodal peak fits of diurnal size distributions at the suburban HKUST supersite and V-mode AMS species  
 624 concentrations (*shaded background*) for organics, nitrate and sulfate (*bottom to top*) in (a) spring, (b) summer, (c) fall and (d) winter in 2011-  
 625 2012; the top panel depicts the diurnal variations of relevant gas-phase pollutants (O<sub>3</sub>, CO, NO<sub>x</sub>, SO<sub>2</sub>) measured at the same site, identical  
 626 plots over each mode

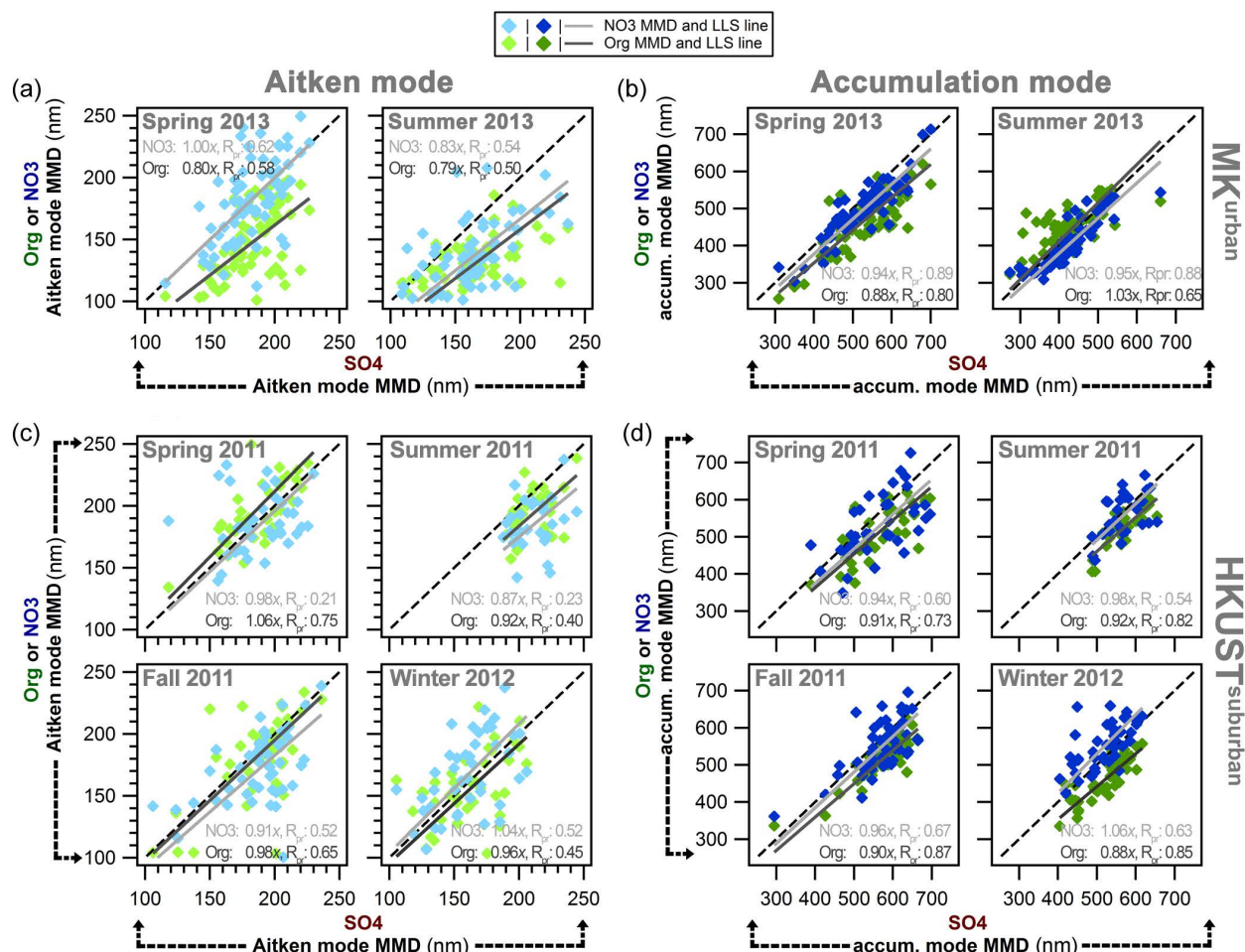




627  
 628 **Figure 3.** Diurnal variation of the fraction of Aitken mode particle mass among total submicron species mass for organics (*bottom*), nitrate  
 629 (*middle*) and sulfate (*top*) at the (a) urban Mong Kong site, and (b) suburban HKUST supersite in different seasons; *based on median*  
 630 *concentrations, seasons denoted by marker color and type of marker symbol*



631  
 632 **Figure 4.** Average and standard deviation of daily fit values of Aitken and accumulation mode particle mass and mass median diameters at  
 633 the suburban HKUST site (*solid bars*) and urban MK site (*hashed bars*). The integrated particle mass is depicted in (a), (b), (c) for the Aitken  
 634 mode, and in (d), (e), (f) for the accumulation mode for sulfate, nitrate, and organics respectively. The mass median diameter is depicted in  
 635 (g), (h), (i) for the Aitken mode and in (j), (k), (l) for the accumulation mode for sulfate, nitrate and organics respectively.



636  
 637  
 638

**Figure 5.** Scatter plots of fitted mass median diameters of organics and nitrate vs. Sulfate for the (a) Aitken mode and (b) accumulation mode at the urban Mong Kok site, and (c) Aitken mode and (d) accumulation mode at the HKUST suburban site